Chapter 28
Octacalcium Phosphate Overgrowth on β-Tricalcium Phosphate Substrate in Metastable Calcium Phosphate Solution

Mayumi Iijima and Kazuo Onuma

Abstract The effects of the particle size of β-tricalcium phosphate (β-$Ca_3(PO_4)_2$; β-TCP) on octacalcium phosphate ($Ca_8(HPO_4)_2(PO_4)_4{\cdot}5H_2O$; OCP) overgrowth on a β-TCP substrate were evaluated under physiological conditions by using two types of substrate; one composed of micrometer-sized particles (micro-TCP substrate) and one composed of nanometer-sized particles (nano-TCP substrate). When the β-TCP substrate was immersed in a simple calcium phosphate solution, it was quickly covered with OCP. The morphology and size of the OCP crystals, as well as the structure, thickness, and crystal density of the overgrown OCP layer, depended on the β-TCP particle size. In case of the micro-TCP substrate, OCP crystals grew directly on the micrometer-sized particles. In case of the nano-TCP substrate, string-like (S) precipitates initially deposited, and then flake-like (F) crystals formed on them. Plate-like (PL) OCP crystals grew on the flake-like crystals; as a result, a three-layer structure (S-layer/F-layer/PL-layer) was formed. Small amounts of tiny OCP crystals and HAp-nanofibers precipitated in the micro-TCP substrate, whereas only HAp-nanofibers precipitated in the nano-TCP substrate. Thus, various types of OCP-overgrown layers were fabricated on β-TCP scaffold. These findings will facilitate the structural design of OCP-coating layers on a β-TCP scaffold.

Keywords Octacalcium phosphate · Coating · Wet chemical method · Overgrowth · β-tricalcium phosphate · Scaffold · Particle size

28.1 Introduction

Both β-TCP and OCP have been proven to have promising osteoconductive characteristics. β-TCP has been applied in the form of granules and three-dimensional (3D) scaffolds (Hench and Polak 2002; Karageogiou and Kaplan 2005; Wang et al.

M. Iijima · K. Onuma (✉)
Biomaterial Research Group, Health Research Institute Central 6, National Institute of Advanced Industrial Science and Technology, Tsukuba, Ibaraki, Japan
e-mail: mayumi-iijima@aist.go.jp; k.onuma@aist.go.jp

K. Endo et al. (eds.), *Biomineralization*,
https://doi.org/10.1007/978-981-13-1002-7_28

2015). The biocompatibility and degradability of conventional micrometer-sized β-TCP powder have been improved by the use of nanometer-sized β-TCP (Zhang et al. 2008; Kato et al. 2016). On the other hand, OCP is a metastable phase of HAp and tends to transform into HAp spontaneously (Brown et al. 1962). The intrinsic properties of OCP are hypothesized to be responsible for its excellent performance in vivo; moreover, implanted OCP granules have provided cores for nucleating multiple osteogenic sites (Suzuki et al. 1991, 2006). The combined usage of β-TCP with its better formability and OCP with its better osteoconductivity would boost the potential of both materials as a bone graft substitute. A practical way to achieve this is coating β-TCP scaffolds with OCP.

The purpose of the present study was to examine OCP formation on a β-TCP substrate in a simple calcium phosphate solution and to evaluate the effect of the particle size of the β-TCP substrate on the overgrowth of OCP under physiological conditions. To achieve this, micrometer- and nanometer-sized β-TCP particles were used to form β-TCP substrate.

28.2 Materials and Methods

Reagent-grade β-TCP powder (Wako, Ltd.) and atomized powder were molded into substrate composed with micrometer-sized particles (0.5–3 μm) (micro-TCP substrate, Fig. 28.1a) and with nanometer-sized particles (<100 nm) (nano-TCP substrate, Fig. 28.1b).

Each substrate section was immersed in a calcifying solution (5 mM $CaCl_2$, 5 mM K_2HPO_4+KH_2PO_4, 50 mM CH_3COONa, pH 6.2, 37 ± 0.5 °C) for required

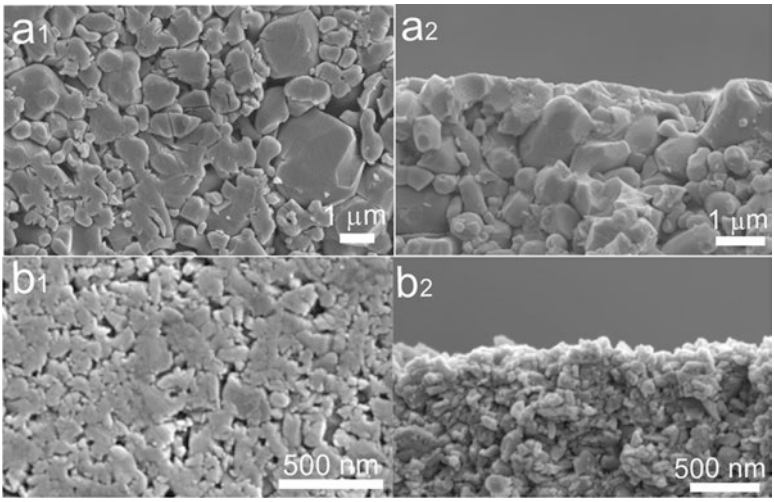

Fig. 28.1 SEM images of the surfaces (a1, b1) and cross sections (a2, b2) of (**a**) micro-TCP substrate and (**b**) nano-TCP substrate before immersion

periods. After the reaction terminated, the substrate was rinsed in Mill-Q water and in 99.5% ethanol and dried in air. The crystals in the overgrown layer and inside the substrate were characterized using powder XRD, microbeam XRD, thin-film in-plane XRD, FE-SEM, and TEM.

28.3 Results and Discussion

28.3.1 Early Stage of Overgrowth

On the micro-TCP substrate (Fig. 28.2), crystal growth started with the formation of sparse island-like aggregates of string-like precipitates, which gradually grew into small flakes (1–10 min) and subsequently increased in size (−30 min). Plate-like OCP crystals grew directly on the β-TCP particles and completely covered the substrate surface after 40 min. Thin-film in-plane XRD of the 40 min overgrown layer exhibits a shoulder peak at 4.7° (2θ), which corresponds to the (100) peak of OCP. It became strong after 60 min. On the nano-TCP substrate (Fig. 28.2), particles with a size of 10–20 nm precipitated after 1 min. These particles fused into strings (3 min), which subsequently formed root-like structure (5 min). The top part of the root-like deposits grew into small flakes (10 min), which completely covered the substrate surface. Thirty minutes overgrown layer exhibits a shoulder peak at 4.7° (2θ). Subsequently, plate-like OCP crystals grew on the thin layer of the flakes (60 min).

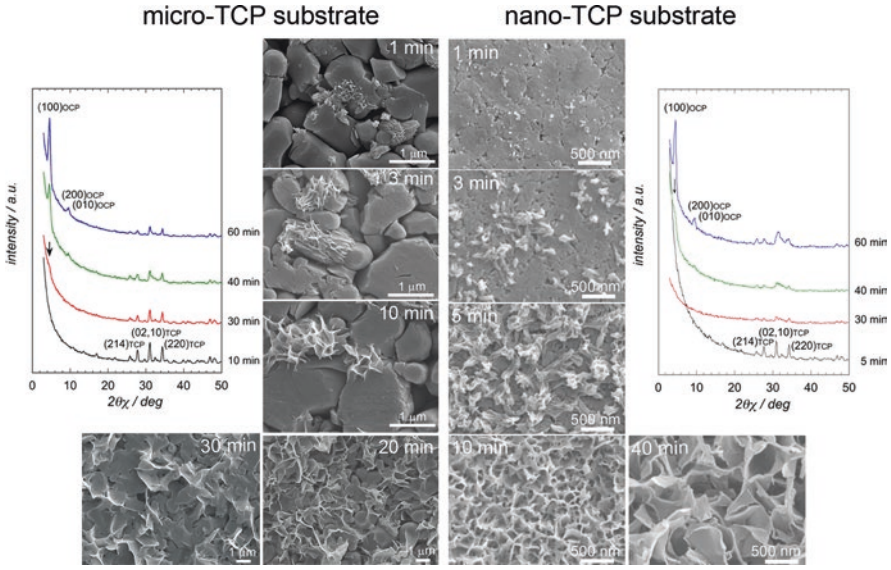

Fig. 28.2 Time-resolved SEM observations and thin-film in-plane XRD measurements of TCP substrate after 1–60 min immersion. Characteristic XRD peaks of OCP (JCPDF 26-1056) and β-TCP (JCPDF 09-0169) are labeled. An arrow indicates shoulder peak of $(100)_{OCP}$ at 4.7° (2θ)

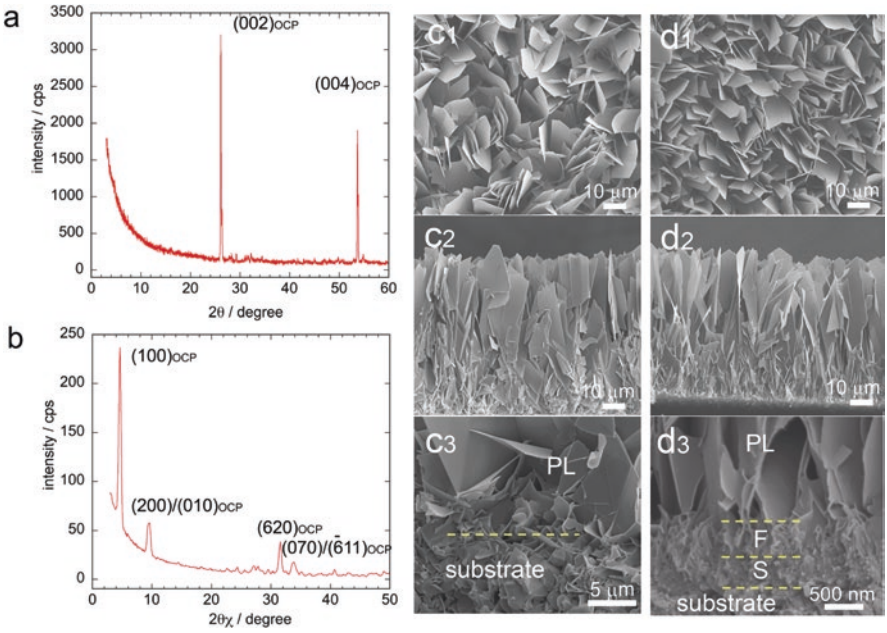

Fig. 28.3 (**a**) Powder XRD, (**b**) thin-film in-plane XRD profiles of micro-TCP substrate and SEM images of (**c**) micro-TCP substrate and (**d**) nano-TCP substrate after 20 h immersion. (c1, d1) top view and (c2, d2) cross-sectional view. (c3) and (d3) are higher magnifications of (c2) and (d2)

28.3.2 Later Stage of Overgrowth

Figure 28.3a, b, respectively, show powder XRD and thin-film in-plane XRD profiles of the micro-TCP substrate after 20 h. Both XRD profiles of the nano-TCP substrate are almost the same. In the powder XRD profile, the (002) and (004) peaks are strong, while the other peaks are very weak. In the thin-film in-plane XRD profile, the peaks in the a-axis direction, (100), (200), and (010), are strong, while the peak in the c-axis direction, (002), is weak. This is due to the c-axial orientation of the OCP crystals on the substrate. The overgrown crystals are identified as OCP by combined analysis of both XRDs.

On both substrates, OCP crystals grew in the same manner. As the immersion period increased, the length of OCP crystals in the c-axis direction increased: 4–6 μm after 60 min, 10 μm after 3 h, 15–20 μm after 5 h, and 66–70 μm after 20 h. In the case of the nano-TCP substrate, plate-like OCP crystals (PL) grew on the layer of small flake-like crystals (F-layer), under which the layer of string-like precipitates (S-layer) had formed, and as a result, a three-layer structure was observed (Fig. 28.3d3). On the contrary, in the case of the micro-TCP substrate, OCP crystals grew directly on β-TCP particles, and no such structure was observed (Fig. 28.3c3).

Inside of the substrates, tiny OCP crystals (Fig. 28.3c3) and small amounts of HAp-nanofibers precipitated in the micro-TCP substrate (Fig. 28.4a, c), whereas

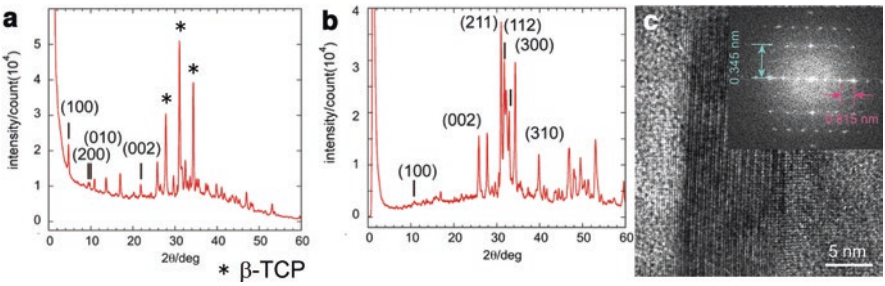

Fig. 28.4 2θ-intensity converted microbeam XRD profile of (**a**) micro-TCP substrate and (**b**) nano-TCP substrate after 20 h immersion. Characteristic XRD peaks of OCP (JCPDF 26-1056) and HAp (JCPDF 09-0432) are labeled, respectively, in (**a**, **b**). (**c**) HR-TEM image of a HAp-nanofiber formed inside of the micro-TCP substrate and its FFT

only HAp-nanofibers were formed in the nano-TCP substrate (Fig. 28.4b). HAp-nanofibers were formed much more in the nano-TCP substrate than in the micro-TCP substrate, and they were localized around particles less than 500 nm in the micro-TCP substrate (Iijima and Onuma 2017). Thus, it was concluded that nano-TCP particles induced the formation of HAp-nanofibers (Onuma and Iijima 2017).

Thus, varying the particle size of the β-TCP had great effect on the early stage of overgrowth and precipitates inside the substrates. Various types of OCP-coating layers were formed on β-TCP substrate. There is a general consensus that the physical properties of the coating layer, i.e., its thickness and topography, affect the in vivo performance of the coated material (Curtis and Wilkinson 1997; Anselme and Bigerelle 2011). These findings will facilitate the structural design of OCP-coating layers on a β-TCP scaffold.

Acknowledgments This study was supported by a Grant-in-Aid for Scientific Research from the Japan Society for the Promotion of Science (JSPS KAKENHI C; 16K04954).

References

Anselme K, Bigerelle M (2011) Role of materials surface topography on mammalian cell response. Int Mater Rev 56:243–266

Brown WE, Smith JP, Lehr JR, Fraier AW (1962) Crystallographic and chemical relation between octacalcium phosphate and hydroxyapatite. Nature 196:1050–1055

Curtis A, Wilkinson C (1997) Topographical control of cells. Biomaterials 18:1573–1583

Hench LL, Polak JM (2002) Third-generation biomedical materials. Science 295:1014–1017

Iijima M, Onuma K (2017) Particle-size-dependent octacalcium phosphate overgrowth on β-tricalcium phosphate substrate in calcium phosphate solution. Ceram Int. https://doi.org/10.1016/j.ceramint.2017.10.167

Karageogiou V, Kaplan D (2005) Porosity of 3D biomaterial scaffolds osteogenesis. Biomaterials 26:5474–5491

Kato A, Miyaji H, Ogawa K, Momose T, Nishida E, Murakami S, Yoshida T, Tanaka S, Sugaya T (2016) Bone-forming effects of collagen scaffold containing nanoparticles on extraction sockets in dogs. Jpn J Conserv Dent 59:351–358

Onuma K, Iijima M (2017) Nanoparticles in β-tricalcium phosphate substrate enhance modulation of structure and composition of an octacalcium phosphate grown layer. Cryst Eng Comm 19:6660–6672

Suzuki O, Nakamura M, Miyasaka Y, Kagayama M, Sakurai M (1991) Bone formation on synthetic precursors of hydroxyapatite. Tohoku J Exp Med 164:37–50

Suzuki O, Kamakura S, Katagiri T, Nakamura M, Zhao B, Honda Y, Kamijo R (2006) Bone formation enhanced by implanted octacalcium phosphate involving conversion into Ca-deficient hydroxyapatite. Biomaterials 27:2671–2681

Wang L, Hu YY, Wang Z, Li X, Li DC (2015) Flow perfusion culture human fetal bone cells in large beta-tricalcium phosphate scaffold with controlled architectures. Ceram Int 41:2654–2667

Zhang F, Chang C, Lin K, Lu J (2008) Preparation, mechanical properties and in vitro degradability of wollastonite/tricalcium phosphate macroporous scaffolds from nanocomposite powders. J Mater Sci Mater Med 19:167–173